DPST-79-128-5/6

^{238}Pu FUEL FORM PROCESSES BIMONTHLY REPORT

MAY/JUNE 1979

Approved by:

R. L. Folger, Research Manager
Hydrogen and Ceramic Technology Division

Publication Date: February 1980

DISCLAIMER

This book was prepared as an account of work sponsored by an agency of the United States Government. Neither the United States Government nor any agency thereof, nor any of their employees, makes any warranty, express or implied, or assumes any legal liability or responsibility for the accuracy, completeness, or usefulness of any information, apparatus, product, or process disclosed, or represents that its use would not infringe privately owned rights. Reference herein to any specific commercial product, process, or service by trade name, trademark, manufacturer, or otherwise, does not necessarily constitute or imply its endorsement, recommendation, or favoring by the United States Government or any agency thereof. The views and opinions of authors expressed herein do not necessarily state or reflect those of the United States Government or any agency thereof.

E. I. du Pont de Nemours & Co. (Inc.)
Savannah River Laboratory
Aiken, SC 29801

PREPARED FOR THE U. S. DEPARTMENT OF ENERGY UNDER CONTRACT DE-AC09-76SR00001

DISTRIBUTION OF THIS DOCUMENT IS UNLIMITED

DISCLAIMER

This report was prepared as an account of work sponsored by an agency of the United States Government. Neither the United States Government nor any agency Thereof, nor any of their employees, makes any warranty, express or implied, or assumes any legal liability or responsibility for the accuracy, completeness, or usefulness of any information, apparatus, product, or process disclosed, or represents that its use would not infringe privately owned rights. Reference herein to any specific commercial product, process, or service by trade name, trademark, manufacturer, or otherwise does not necessarily constitute or imply its endorsement, recommendation, or favoring by the United States Government or any agency thereof. The views and opinions of authors expressed herein do not necessarily state or reflect those of the United States Government or any agency thereof.

DISCLAIMER

Portions of this document may be illegible in electronic image products. Images are produced from the best available original document.

CONTENTS

FOREWORD 5

GENERAL-PURPOSE HEAT SOURCE PROCESS DEMONSTRATION 7

Fabrication Tests of GPHS Fuel Forms 7

Full-scale fabrication tests of General-Purpose Heat Source (GPHS) fuel forms continued in the SRL Plutonium Experimental Facility (PEF) as four additional pellets (GPHS Pellets 5-8) were hot pressed. GPHS pellets fabricated by the reference process were dimensionally and structurally stable during and after final heat treatment.

Microstructural Analyses of GPHS Pellets 3, 4, and 5 14

Microstructural studies confirmed that centerline GPHS process conditions produce pellets with a homogeneous microstructure and a uniform density.

PuFF Furnace Racks for GPHS Fuel Production 22

Because of the potential for excessive metal creep in existing furnace racks, the racks were considered unacceptable for GPHS fuel production in the PuFF. To eliminate metal creep, racks containing some ceramic components were designed to operate at 1600°C in an oxygen atmosphere for more than 100 hours.

MULTI-HUNDRED WATT PROCESS SUPPORT 27

Statistical Analysis of MHW Production Data 27

The four-key variables previously identified (shard sintering temperature, hot press load, hot press temperature, and load ramp) were found to correlate with production sphere fracture tendency and bulk density.

REFERENCES 40

FOREWORD

This report is one of a series to summarize progress in the Savannah River ^{238}Pu Fuel Form Program. This program is supported primarily by the DOE Advanced Nuclear Systems and Projects (ANSAP) and also by the Division of Military Applications (DMA).

Goals of the Savannah River Laboratory (SRL) program are to provide technical support for the transfer of DASMP and DMA ^{238}Pu fuel form fabrication operations from Mound Laboratory to new facilities at the Savannah River Plant (SRP), to provide the technical basis for ^{238}Pu scrap recovery at SRP, and to assist in sustaining plant operations. This part of the program includes:

Demonstration of processes and techniques, developed by the Los Alamos Scientific Laboratory (LASL) for production at SRP. Information from the demonstration will provide the technical data for technical standards and operating procedures.

Technical Support to assist plant startup and to ensure continuation of safe and efficient production of high-quality heat-source fuel.

Technical Assistance after startup to accommodate changes in product and product specifications, to assist user agencies in improving product performance, to assist SRP in making process improvements that increase efficiency and product reliability, and to adapt plant facilities for new products.

GENERAL-PURPOSE HEAT SOURCE PROCESS DEMONSTRATION

FABRICATION TESTS OF GPHS FUEL FORMS

Full-scale fabrication tests of General-Purpose Heat Source (GPHS) fuel forms continued in the Savannah River Laboratory (SRL) Plutonium Experimental Facility (PEF) as four additional pellets (GPHS Pellets 5-8) were hot pressed. The quality of the pellets continued to improve with fabrication experience. Pellets fabricated by the reference process were dimensionally and structurally stable during and after final heat treatment. Hot pressing conditions were adjusted to permit pellet removal from the die by extrusion. Three of the first four pellets in the initial fabrication tests had to be cut from the die.[1]

Fabrication Conditions

Process condtions for fabricating GPHS Pellets 5-8 are summarized in Tables 1-4. The same conditions were used for all pellets to process the as-received powder into granules (Table 1). Intentional variations were made in the process conditions for granule sintering, hot pressing, and final heat treatment. These conditions are given in Tables 2-4 and are discussed below.

For fabricating GPHS Pellets 5-8, process conditions from ^{16}O-exchange through granulation are identical to those described in the flowsheet currently used for fabricating fuel forms for the Multi-Hundred Watt (MHW) Heat Source in the Plutonium Fuel Form (PuFF) Facility. On the basis of results of fabricating GPHS Pellets 1-8, these conditions appear to be satisfactory for production of GPHS fuel forms.

GPHS Pellets 5, 7, and 8 were made from the reference shard mixture with the reference die design. The goal of the fabrication test for GPHS Pellets was to adjust hot pressing conditions to minimize reduction of the PuO_2 and corrosion of the die wall. In this test, heating to the hot pressing temperature was 2 to 5 times faster than in previous tests (10 min versus 20 to 48 min with GPHS Pellets 1-4) and a faster load ramp (5 min versus 10 min) was used. Also, the time at maximum temperature and load was minimized by initiating cooling and load removal as soon as die closure was noted.

TABLE 1

GPHS Process Conditions Used in PEF Tests

^{16}O Exchange (simulated)	4 hr @ 800°C
Outgas	1 hr @ 1000°C
Ball Mill	12 hr @ 100 rpm
Compact	58,000 psi
Granulate	<125 μm
Sinter Shard	See Table 2
Hot Press	See Table 3
Heat Treatment	6 hr @ 1000°C and 6 hr @ 1525°C

TABLE 2

Shard Mixture and Sintering Conditions for GPHS Pellets

	Description of Mixture		
GPHS Pellet No.	Composition of Mixture, %	Temp, °C	Time, hr
5	60	1100	6
	40	1600	6
6	86	1300	9
	14	1450	6
7	60	1100	6
	40	1600	6
8	60	1100	6
	40	1600	6

TABLE 3

Hot Pressing Conditions for GPHS Pellets

	GPHS Pellet No.			
	5	6	7	8
Preload, lb	200	200	200	200
Heating				
Time to 1100°C, min	4	4	3	3
Max Temp, °C	1510	1550	1530	1530
Time to Max Temp, Min	10	8	8	8
Load				
Temp of Initiation, °C	1370	1500	1360	1360
Max Load, lb	2600	2600	2600	2600
Ramp, min	5	5	5	5
Time Between Initiation of Heat and Load, min	6	8	4	4
Time to Die Closure after Max Load	1	4	2	10
Time at Max Load and Temp after Closure	2	5	5	4

TABLE 4

Final Heat Treatment Conditions for GPHS Pellets

	GPHS Pellet No.			
	5	6	7	8*
Heat Rate, °C/hr	<200	<200	<200	<200
Intermediate Hold				
Temp, °C	1000	1000	--	--
Time, hr	6	6	--	--
Maximum Hold				
Temp, °C	1525	1525	1525	1525
Time, hr	6	6	6	6
Cooling Rate, °C/hr	<200	<200	<200	<200

* Planned conditions for final heat treatment.

GPHS Pellet 7 was fabricated using the current best estimate of centerline process conditions. GPHS Pellet 8 was the first attempt to produce a pellet of relatively high density to determine whether GPHS pellets can be fabricated to the maximum expected density [86% theoretical density (TD)] without fracturing.

Final heat treatment was also modified for GPHS Pellet 7. The intermediate hold condition of 1000°C for 6 hours on heating was eliminated (Table 4) to shorten the overall time for process operation. Both Los Alamos Scientific Laboratory (LASL) and SRL experimenters believe that the intermediate hold serves no useful function. Future microstructural analysis on GPHS Pellet 7 is expected to confirm this belief.

GPHS Pellet 6 was fabricated in the same die that was used for Pellet 5. For GPHS Pellet 6 a shard mixture of 86% sintered at 1300°C and 14% sintered at 1450°C (Table 2) was used. This hot pressing test was made to use up remnant shards and to evaluate the effect of shard properties on hot pressed fuel forms.

Pellet Removal from Die

GPHS Pellets 5, 7, and 8 were extruded from the die using the cold press in the PEF. No pressure was observed on the pressure gage of the cold press during extrusion of GPHS Pellets 5 and 7. A slight pressure of up to 200 lb was observed intermittently during removal of GPHS Pellet 8. GPHS Pellet 6 had to be cut from the die. In previous full-scale tests (GPHS Pellets 1-4), only GPHS Pellet 2 was successfully extruded from the die.

The successful extrusion of GPHS Pellets 5, 7, and 8 from the die is attributed to the faster heat-up rate and load ramp during hot pressing. The time available for the PuO_2 - die interaction was reduced. Calculation of the as-pressed stoichiometry of the various pellets showed that the oxygen-to-plutonium ratios for GPHS Pellets 5-8 was 1.93 compared to 1.85 to 1.90 for the other pellets (Table 5). The need to cut GPHS Pellet 6 from the die is attributed to the additional corrosion which resulted from using the same die as that used to hot press GPHS Pellet 5. The slight pressures observed during the extrusion of GPHS Pellet 8 from the die presumably developed because a higher PuO_2 charge to the die increased the time for die closure, increased the PuO_2 - die interaction, and hence increased die wall corrosion. Fabrication of GPHS Pellet 8 was the first attempt to produce a high-density (86% TD) pellet.

TABLE 5

Summary of GPHS Pellet Characteristics

GPHS Pellet No.	Condition	Diameter, in.	Length, in.	Weight, g	Density, % TD	O/M
2*	As-pressed	1.065	1.066	146.683	82.3	1.89
	Heat Treated	1.064**	1.055	147.630	>83.8†	
	Difference	-0.1%	-1.0%	0.947	1.5	
3*	As-pressed	1.072	1.074	145.714	80.4	1.85
	Heat Treated	1.065**	1.066	146.999	>82.4†	
	Difference	-0.7%	-0.7%	1.285	2.0	
4†	As-pressed	1.100	1.104	151.450	81.8	1.90
	Heat Treated	1.096	1.100	152.367	83.3	
	Difference	-0.4%	-0.4%	0.917	1.5	
5†	As-pressed	1.095	1.097	151.707	84.3	1.93
	Heat Treated	1.092	1.093	152.351	84.3	
	Difference	-0.3%	-0.4%	0.644	1.0	
6††	As-pressed	1.107	1.107	152.069	81.1	1.90
	Heat Treated	¶	1.099	152.934¶¶	¶	
	Difference		-0.7%			
7†	As-pressed	1.093	1.099	152.864	84.0	1.93
	Heat Treated	1.089	1.096	153.470	85.2	
	Difference	-0.4%	-0.3%	0.606%	1.2%	
8†	As-pressed	1.098	1.112	155.582	83.7	$\geq$1.88
	Heat Treated					
	Difference					

* Shard mixture: 60% sintered at 1150°C and 40% sintered at 1450°C; pellet geometry: right circular cylinder.

** Pellet fractured; diameter measured and density calculated from reassembled pieces.

† Reference shard mixture and reference geometry.

†† Remnant shards and reference geometry.

¶ Pellet was sectioned longitudinally prior to final heat treatment.

¶¶ Pellet weight calculated based on weight gain measured for half pellet.

Pellet Characteristics

Quality of pellets produced in these full-scale fabrication tests continued to improve with experience. All the pellets produced in these recent tests (GPHS Pellets 4-8) were integral with no apparent surface cracks as pressed. In addition, GPHS Pellets 5 and 7 were integral after final heat treatment but both contained several hairline cracks. Pellet characteristics are summarized in Table 5.

GPHS Pellet 6 was sectioned in half longitudinally before final heat treatment to compare as-pressed and heat-treated microstructures. Several internal cracks were observed on sectioned surfaces. The cracks widened somewhat during final heat treatment, but the half pellet remained integral.

The as-pressed density of GPHS Pellet 8 was lower than anticipated, i.e., 83.7% TD instead of >85% TD expected from the weight of PuO_2 charged to the die and the expected volume of the die cavity at closure. The lower density resulted from an increase in pellet volume caused by corrosion of the die material at the PuO_2-graphite interface. The diameter and length of GPHS Pellet 8 were 0.005 in. and 0.004 in., respectively, greater than the original dimensions of the die. The additional corrosion may have occurred because additional time was required to obtain die closure (Table 3) with the larger PuO_2 charge to the die.

All the GPHS pellets made from the reference shard mixture (GPHS Pellets 4, 5, and 7) exhibited excellent dimensional stability during final heat treatment (Table 5). Linear shrinkage in diameter and length were limited to 0.3 to 0.4% (0.003 to 0.004 in.). Axial shrinkage of GPHS Pellet 6 was 0.007 in. (about twice that observed for GPHS Pellets 4, 5, and 7). The different shard mixture and sintering temperatures used to make GPHS Pellet 6 may have caused the increased shrinkage.

Microstructural characterization of GPHS Pellets 3, 4, and 5 is discussed in a later section of this report.

Low-Temperature Reoxidation

Little or no reoxidation was observed in as-pressed GPHS pellets that were stored in a graphite container that was vented to the PEF atmosphere containing up to 1000 ppm oxygen. LASL has recommended storage of as-pressed pellets for 16 hours in vented graphite containers to permit reoxidation to occur.[1] However, the data obtained on GPHS Pellets 5, 6, and 7 (Table 6) show only a slight weight gain (due to reoxidation) after exposures of up to 90 hours. These data suggest the 16-hour storage in graphite may not serve any useful purpose. Additional tests are planned to determine whether final heat treatment can be initiated immediately upon removal of the pellet from the die.

TABLE 6

Low-Temperature Reoxidation of GPHS Pellets

GPHS Pellet No.	Condition	Wt, g	O/M
5	As-pressed	151.707	1.929
	25 hr	151.940	1.954
	90 hr	151.999	1.961
	Heat treated	152.351	2.000
6	As-pressed	152.069	1.905
	20 hr	152.133	1.912
	44 hr	152.139	1.912
	Heat treated	80.054*	2.00
7	As-pressed	152.864	1.933
	17 hr	152.865	1.933
	Heat treated	153.470	2.000

* Only 1/2 of pellet heat treated; O/M based on as-pressed, half-pellet weight of 79.638 at 44 hr.

Current Centerline Conditions

Integral GPHS fuel forms with a desirable uniform microstructure have been fabricated in the PEF using the LASL flowsheet as modified by SRL. A current best estimate of centerline conditions for producing GPHS fuel forms include:

- Powder receipt through granulation identical to MHW process conditions (Table 1).
- Granule sintering temperatures and shard mixture identical to the LASL flowsheet (i.e., 60% sintered at 1100°C and 40% sintered at 1600°C).
- Hot press cycle as shown in Table 7.
- Final heat treatment cycle identical to the one used for GPHS Pellet 7 (Table 4).

Changes are expected in these centerline conditions as additional data become available. Such changes may optimize conditions for process control and product improvement or simplify operations for production in the PuFF Facility.

TABLE 7

GPHS Hot Press Cycle

Operation	Time, min
Preload	
Move rams to contact punches	3
Increase 60 to 200 lb	5
Heat	
Ambient to 1350°C	4
1350°C to 1530°C	4
Load	
Initiate at 1350°C	
Increase 200-2600 lb	5
Hold 5 min after closure	5-15
Decrease 2600-50 lb	10
Cool	
1530 to ~1000°C	10
Shut off power	
Total Elapsed Time	32-42

Program

Full-scale fabrication tests will continue with the reference shard mixture and pellet shape. The near-term goal is to demonstrate that acceptable GPHS fuel forms can be fabricated reproducibly using the current best estimate of centerline process conditions. Longer-range goals are to (1) determine the effect of key process variables, (2) optimize centerline conditions, and (3) set limits for subsequent production in the PuFF Facility.

MICROSTRUCTURAL ANALYSES OF GPHS PELLETS 3, 4, AND 5

Microstructural analyses confirmed that centerline GPHS process conditions, developed by LASL ("General-Purpose Heat Source Project - Preliminary LASL Fuel Flow Process: GPHS Program Review, Los Alamos Scientific Laboratory," January 30, 1979), and modified for use in the PEF (J. W. Congdon's Trip Report, GPHS Technology Transfer Meeting, LASL, April 17-20, 1979, dated May 29, 1979), produced a homogeneous microstructure and uniform

density distribution in GPHS Pellet 4. However, variations in the process parameters away from centerline conditions (feed material and hot pressing parameters) resulted in a radial density gradient of about 7% TD in GPHS Pellet 3. Microstructural examination of GPHS Pellet 5 revealed large (1000 to 2000 m), high-density aggregates throughout an otherwise homogeneous microstructure.

This study is part of a continuing program of microstructural characterization of GPHS pellets that are being fabricated in the PEF. The primary goals of the microstructural analysis of GPHS pellets are to (1) determine process conditions that yield a homogeneous microstructure and uniform density distribution and (2) determine effects of deviations from centerline conditions on the microstructure and fracture tendency. In this report we discuss the microstructural characteristics of GPHS Pellets 3, 4, and 5.

The fabrication conditions and densities of GPHS Pellets 3, 4, and 5 are given in Table 5. After heat treatment, radial sections of GPHS Pellets 3 and 4 and longitudinal sections from both ends of GPHS Pellets 4 and 5 were prepared by standard metallographic techniques. The specimens were examined with the metallograph in the as-polished and acid-etched conditions.

GPHS Pellet 3

The bulk density of GPHS Pellet 3 after heat treatment was 82.4% TD slightly lower than the reference GPHS density of 84 to 85% TD. As shown in the low-magnification micrograph in Figure 1, a significant density differential (about 7% TD) exists in the radial cross section. The higher-density surface region (86% TD) extends approximately 0.15 in. into the interior. Metallographic densities in the interior region of GPHS Pellet 3 average about 79% TD. This density variation is accompanied by a variation in microstructure as shown in Figure 2. The shard structure and large intershard pores were retained in the higher-density surface. However, the interior pore structure included pore channels at most of the shard boundaries.

GPHS Pellet 4

GPHS Pellet 4, which was fabricated using centerline process conditions, had a bulk density of 83.3% TD after heat treatment. Radial and longitudinal cross sections (Figure 3) showed that the density and microstructure throughout the pellet were relatively homogeneous (Figures 4 and 5). Slightly lower densities (about 2% lower) were observed near the radiused corners of the pellet (Figure 6). Surface tensile cracks (about 0.1 inch long) were also observed in GPHS Pellet 4 (Figure 3).

In addition, a bimodal grain size distribution was revealed in GPHS Pellet 4 by acid etching (Figure 7). The mean grain size was about 30 μm within the high-fired shards and about 10 μm within the low-fired shards.

GPHS Pellet 5

The bulk density of GPHS Pellet 5 was 84.3% TD after heat treatment. As shown in Figure 8, the microstructure was relatively homogeneous except for numerous high-density regions (about 1000 to 2000 μm diameter). These regions were presumably caused by high-density aggregates which formed during storage of the shards. Self-heat temperatures during storage were apparently sufficient to initiate sintering between the shards and create large, dense aggregates. On the basis of the observed high-density regions, we recommend that shards be screened (to <125 μm) immediately prior to hot pressing to eliminate formation of high-density aggregates during storage.

Surface

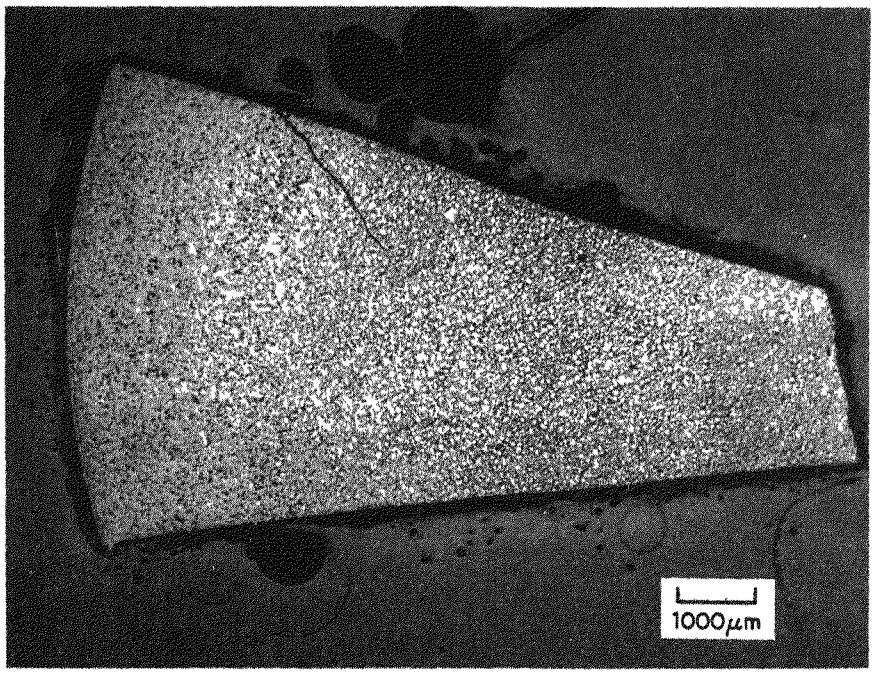

Center

FIGURE 1. Radial Cross Section of GPHS Pellet 3. Bulk Density = 82.4% TD. Heat treated, as polished.

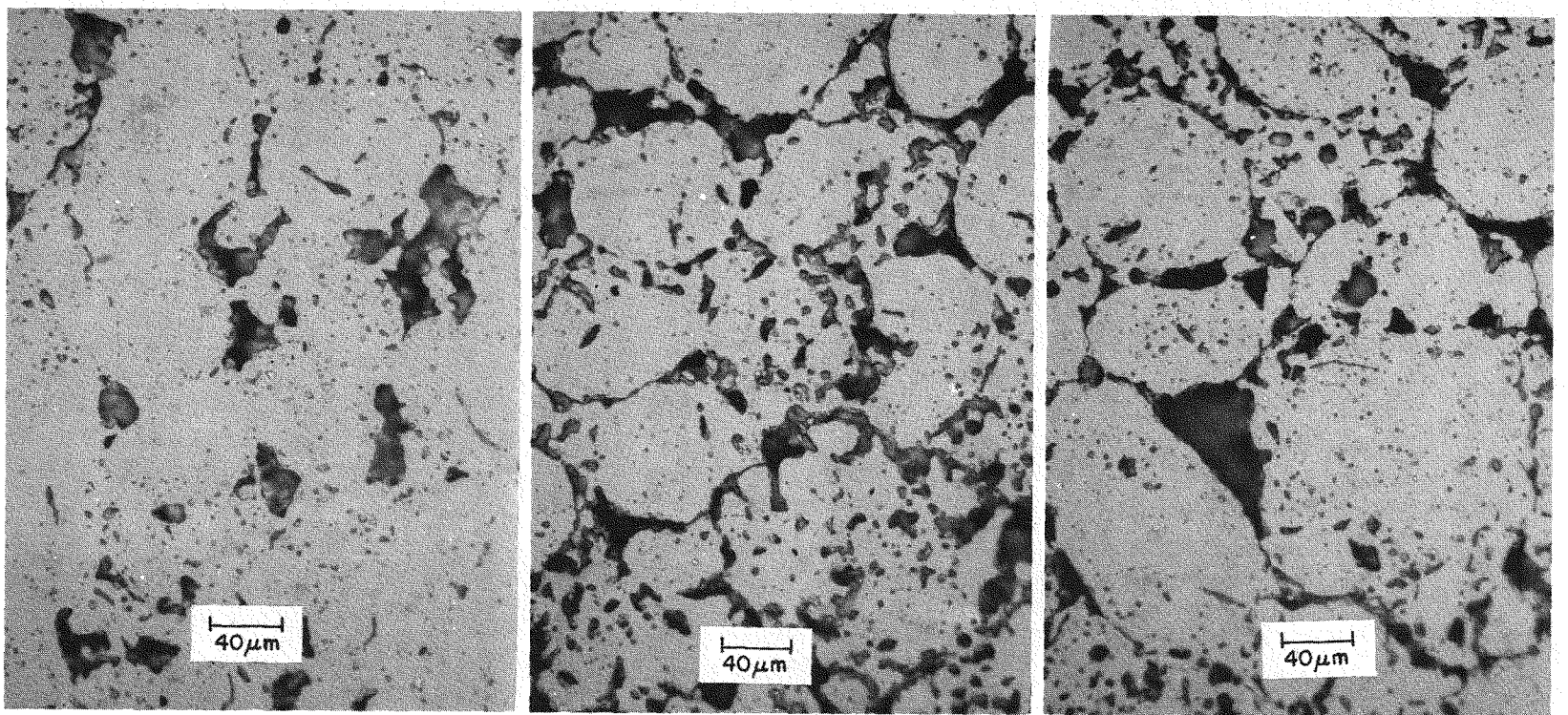

Surface
86% TD

79% TD

Center
80% TD

FIGURE 2. Microstructure of GPHS Pellet 3 along Radial Axis. Heat treated, as polished.

End

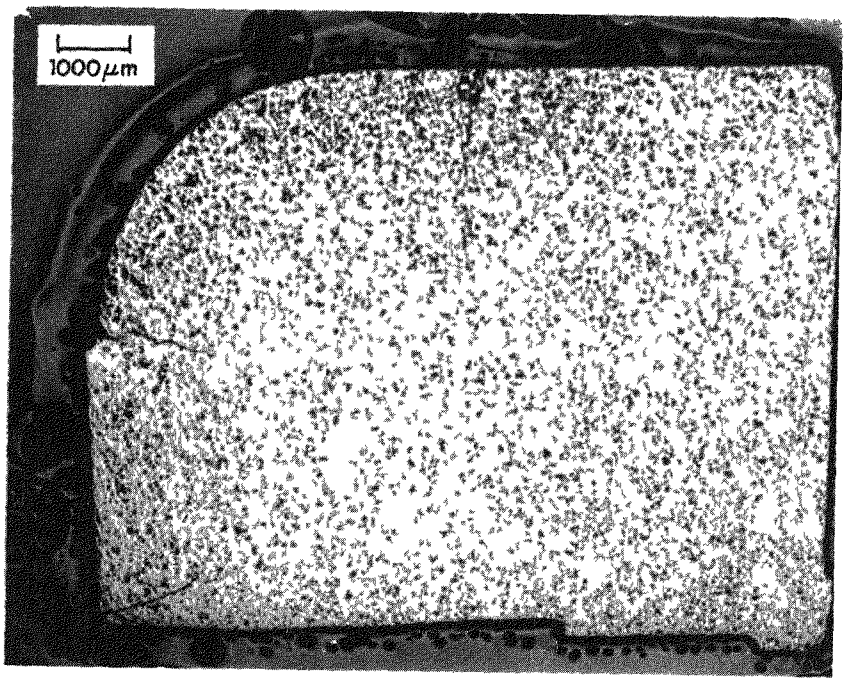

Center

FIGURE 3. Longitudinal Cross Section of GPHS Pellet 4. Bulk density = 83.3% TD. Heat treated, as polished.

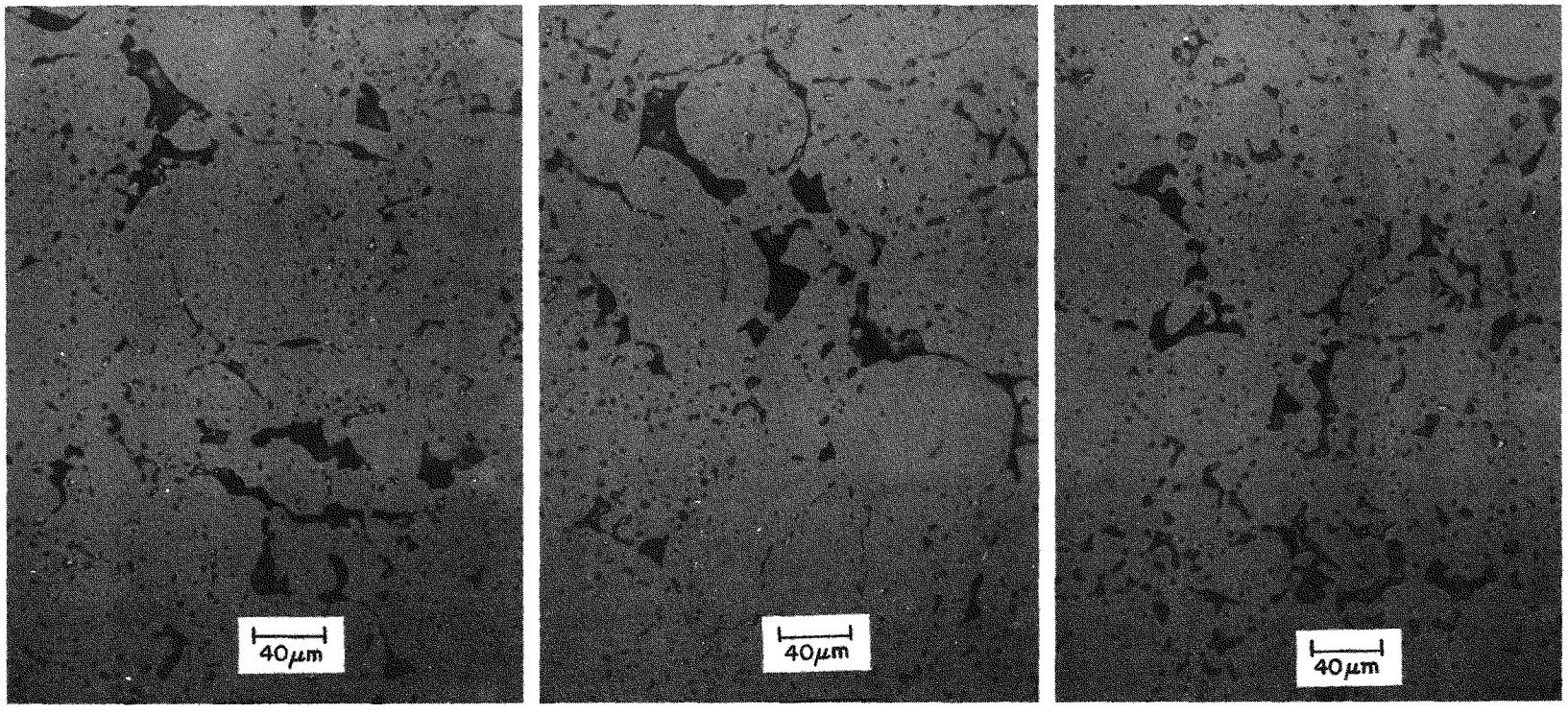

Surface
86% TD

Interior
86% TD

Center
85% TD

FIGURE 4. Microstructure of GPHS Pellet 4 along Radial Axis. Heat treated, as polished.

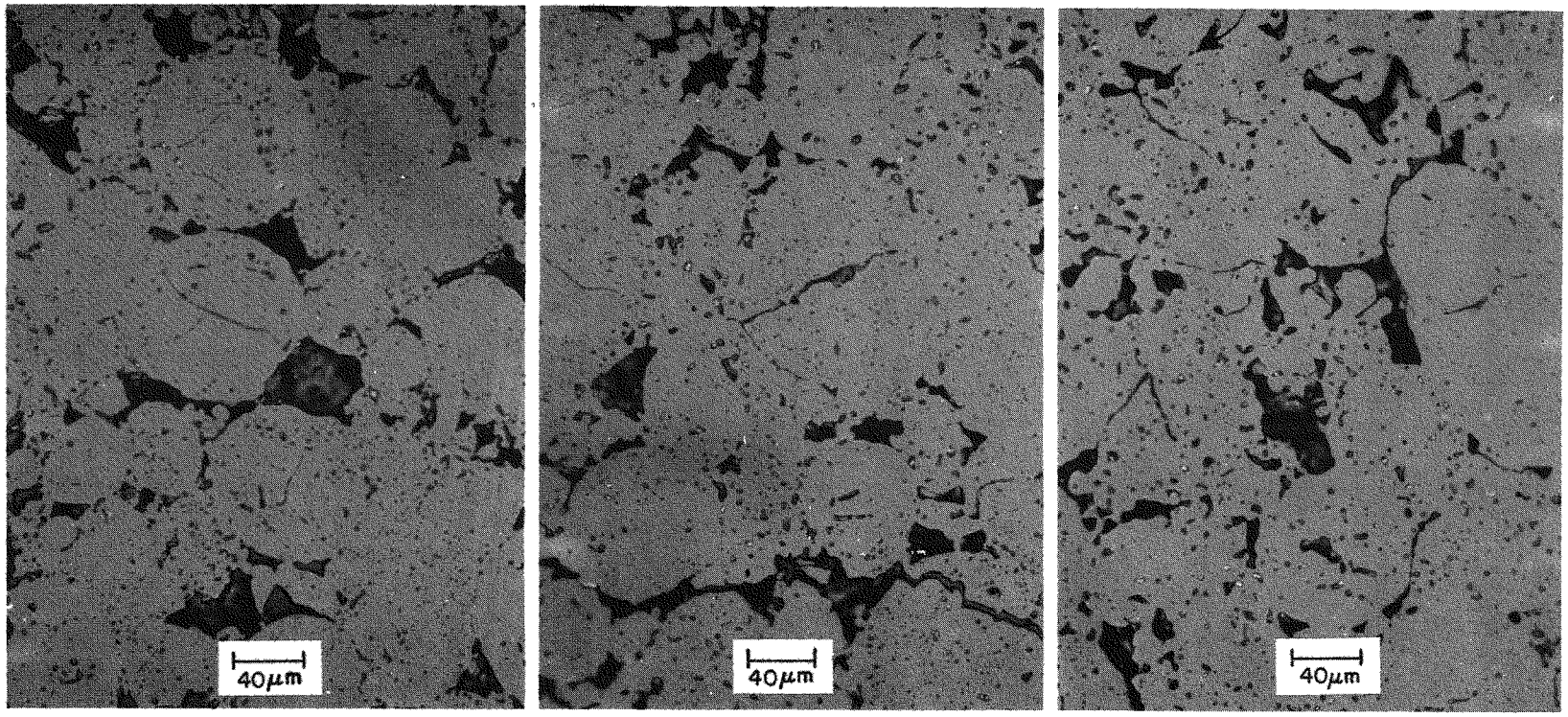

End
84% TD

85% TD

Center
85% TD

FIGURE 5. Microstructure of GPHS Pellet 4 along Longitudinal Axis. Heat treated, as polished.

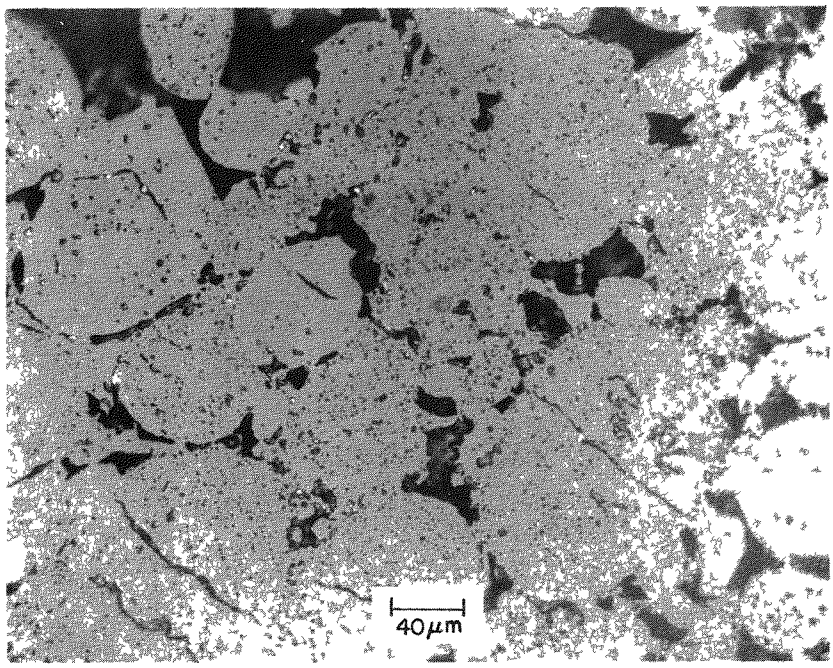

FIGURE 6. Microstructure at Radiused Corner of GPHS Pellet 4. Heat treated, as polished, 83% TD.

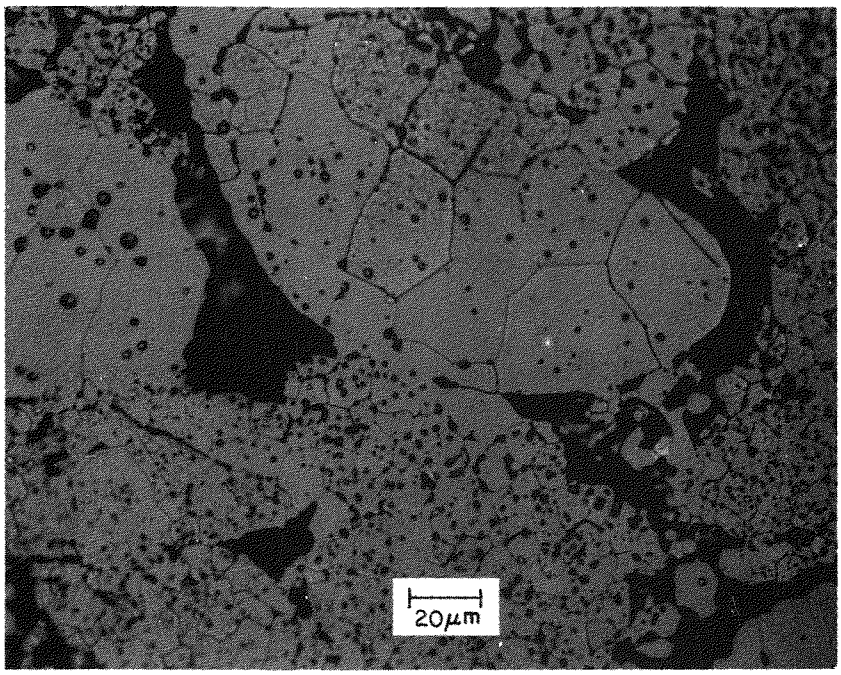

FIGURE 7. Bimodal Grain-Size Distribution in GPHS Pellet 4. Heat treated, grain-boundary etched.

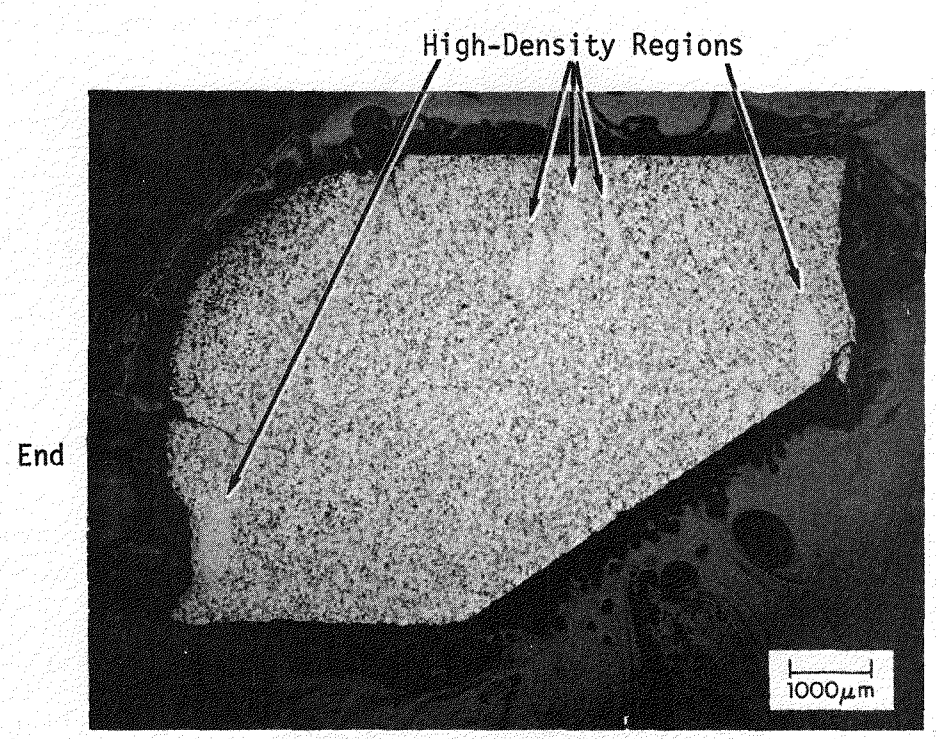

FIGURE 8. Longitudinal Cross Section of GPHS Pellet 5 Showing High-Density Regions

PuFF FURNACE RACKS FOR GPHS FUEL PRODUCTION

Because of the potential for excessive metal creep in the existing furnace racks used in the PuFF facility, the racks were considered unacceptable for GPHS fuel production. To limit metal creep, racks containing some ceramic components were designed to operate at 1600°C in an oxygen atmosphere for more than 1000 hours.

The SRP Plutonium Fuel Form (PuFF) Facility will begin production of a $^{238}PuO_2$ fuel form in 1980 for use in the GPHS. This fuel form is made by hot pressing a mixture of shards (granules) presintered at 1600°C (40%) and 1100°C (60%). The existing support racks for the shard sintering furnace in the PuFF Facility were designed for a maximum temperature of only 1440°C. Therefore to avoid excessive creep at higher temperatures, new furnace racks had to be designed that could operate at 1600°C in an oxygen atmosphere for more than 1000 hours.

A preliminary furnace rack and tray assembly design called for metal racks and trays (ceramic racks were considered unreliable because of the possibility of fracture) constructed of the alloy ZGS Pt-10% Rh. This design (Figure 9) had the following features:

- Cross sectional areas of critical strength members in the rack shelf were large enough to reduce the maximum expected stresses in the critical members (the ring and cross bars) to approximately 0.25 kg/mm^2. (On the basis of extrapolated creep and rupture data [Figure 10] the rack shelf was expected to have a useful life exceeding 1000 hours.)

- Aluminum oxide discs were inserted between the pellet trays and shelves to prevent shelf welding.

- The number of trays was reduced from four to three to improve handling of GPHS pellets and to accommodate the aluminum oxide discs and the increased shelf thickness.

To qualify the ZGS Pt-10% Rh alloy for use in the furnace rack and tray assembly, a creep (deformation) test was made under the expected furnace operating conditions (0.25 kg/mm^2 load at 1600°C). However, under these conditions the alloy deformed rapidly (Figure 11) with a linear creep rate (second stage) of 1.3×10^{-2} %/hr. Rupture occurred after only 631 hours. With this deformation behavior the metal racks as designed would have been unusable after only 100 hours of use.

The initial design of the racks was modified to substantially reduce creep in the critical strength members. In the modified design (Figure 12), stresses in the high-stress components were reduced to ≤ 0.1 kg/mm^2 by increasing the cross section of the beams and by replacing the two notched crossing beams with three parallel channels. Alumina reinforcing rods were added to the tray supports to relieve stresses in the ZGS Pt-10% Rh alloy support members after deformation of only about 0.005 in. This hybrid design combines the strength and creep resistance of alumina with the durability of ZGS Pt-10% Rh.

Engineering drawings of the modified design have been submitted to SRP, and a project to procure two furnace racks is being written. Creep rate and rupture tests are being continued to obtain data over the range of conditions of interest.

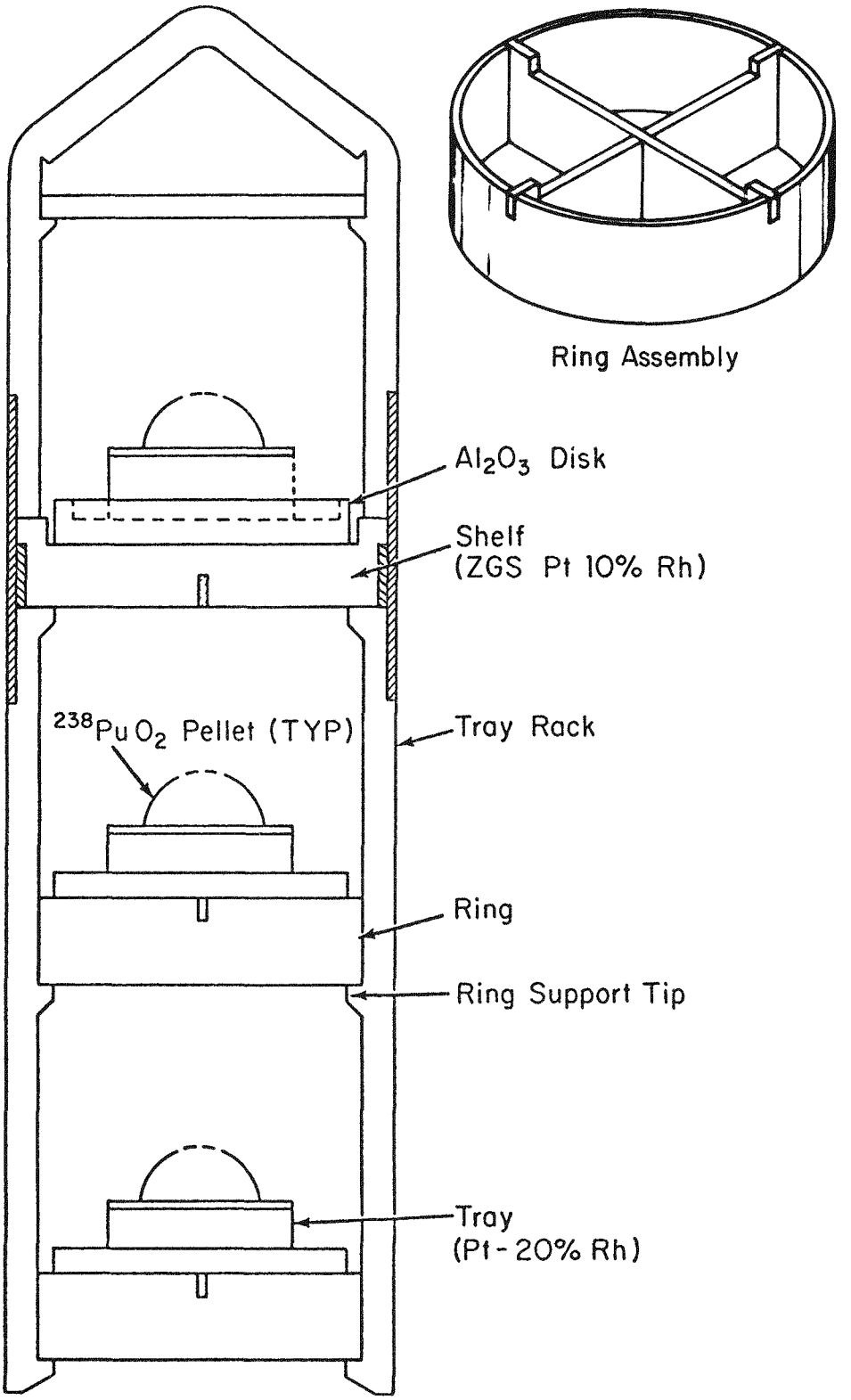

FIGURE 9. PuFF Furnace Rack-and-Tray Assembly

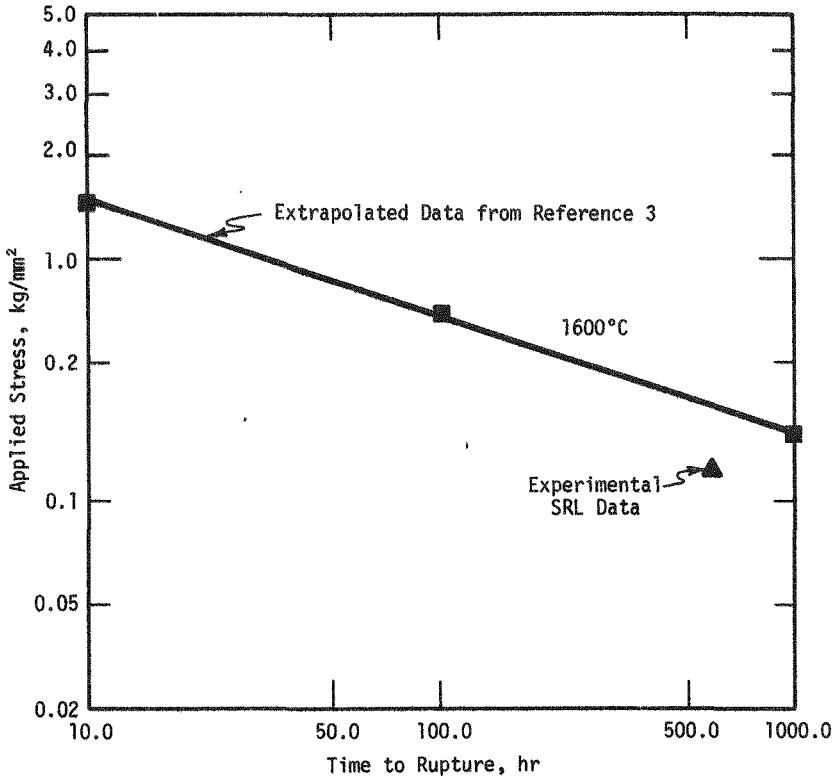

FIGURE 10. Design Stress Levels for Rack and Tray Assembly Compared to Stress Rupture Data for ZGS Pt-10% Rh

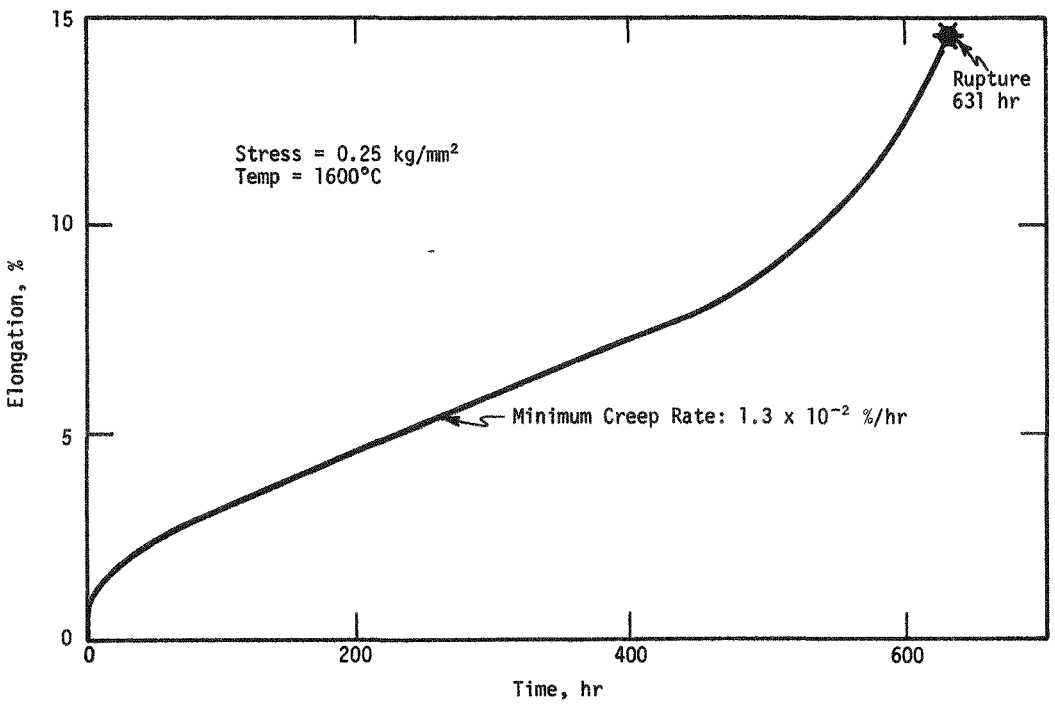

FIGURE 11. Elongation versus Time for High-Temperature Creep of ZGS Pt-10% Rh

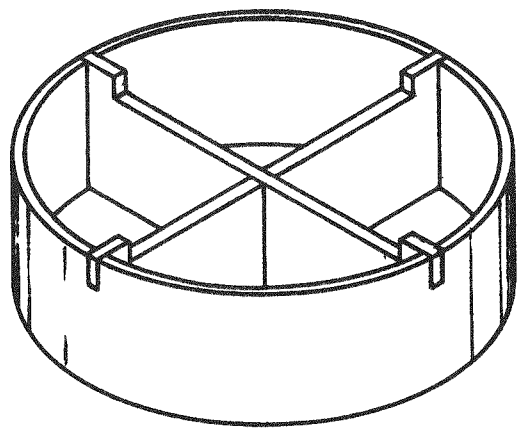

Initial Design

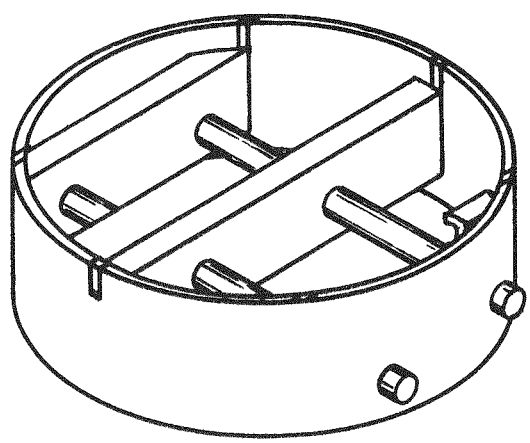

Modified Design

FIGURE 12. Tray Support Rings for Support Racks for PuFF Vertical Furnaces

STATISTICAL ANALYSIS OF MHW PRODUCTION DATA

Background

A statistical analysis of all MHW production data through Sphere 58 has been completed. The four-key variables previously identified (shard sintering temperature, hot press load, hot press temperature, and load ramp) were found to correlate with sphere fracture tendency and both as-pressed and heat-treated bulk densities. On the basis of this analysis, the centerline conditions shown in Table 8 are recommended for the key MHW fabrication variables.

TABLE 8

Centerline Conditions for MHW Heat Source Fabrication

Variable	Recommended	Current Centerline
Shard Sintering Temperature, °C	1315	1310 - 1315
Hot Press Load, lb	2575	2500
Hot Press Temperature, °C	1555	1545
Rate, lb/min	241	241

The analysis also emphasized the need for closer and more accurate control of production variables. Statistical evaluation of production data was only possible because of considerable fluctuation in supposedly constant fabrication conditions. While this turned out to be beneficial in relating final sphere properties to values of the key variables, it underscored the need to improve control of critical parameters. In particular, we recommend that the shard sintering temperature be controlled to ± 5°C.

The statistical analysis of production data was the final step in a program to relate sphere properties (particularly fracture resistance and dimensional stability) to fabrication conditions. Previous characterization of experimental parametric pellets and spheres identified the key processing variables as shard sintering temperature, hot press load, hot press temperature, and load ramp. The objective of analyzing the production data was to evaluate these variables and others for interactions (synergistic effects) and for practical limits.

Scope of Statistical Analysis

Table 9 lists the sphere properties that were investigated for correlation with fabrication variables. Fracture tendency, heat-treated density, and as-pressed density were found to correlate with some production variables as already mentioned. No correlations were found for as-pressed stoichiometry and polar or equatorial shrinkage on heat treatment, although this result may only reflect insufficient or inadequate data. Table 10 lists the process variables evaluated using the production data. Correlations were obtained only with the four-key variables found previously which may again simply indicate that the data were inadequate to detect correlations, perhaps because the fluctuations in the production variable were too small to give rise to noticeable effects.

The statistical analysis showed that sphere properties are controlled by strong interactions among the four-key variables. Consequently the effect of any of the four variables depends on the settings of at least two others. It is for this reason that in the past, correlations with single variables such as hot press temperature or pressure have been so elusive.

TABLE 9

Sphere Properties Evaluated for Correlation With Fabrication Variables

Fracture tendency

Heat-treated density

As-pressed density

As-pressed stoichiometry

Polar shrinkage

Equatorial shrinkage

TABLE 10

Fabrication Variables Evaluated for Correlation With Sphere Properties or Each Other

Shard sintering temperature

Hot press load

Hot press temperature

Total time at maximum hot press temperature

Load ramp

Time to close die

Total time at temperature after die closure

Die charge weight

Statistical Model

The correlations have been quantified into a mathematical model so that density and fracture response can be calculated from the settings of the four-key variables using a polynominal equation (Equations 1-3). Table 11 compares the observed and calculated density and fracture response for production Spheres 13 to 58 for which appropriate data were available. As expected from the standard error of the analysis for density (0.83% TD) the agreement between calculated and measured densities is good. Sphere density was determined from the measured sphere dimensions and weight. Sphere fracture tendency was measured on a scale from 1 to 3 in which 3 was fracture during heat treatment, 2 was fracture on standing after heat treatment but before encapsulation, and 1 was no fracture through encapsulation. The fracture columns in Table 11 show that spheres with a calculated fracture tendency less than about 1.5 should survive unfractured through encapsulation.

Application of Statistical Model

The model (Equations 1-3) was applied to two spheres made subsequent to Sphere 58 and it successfully predicted the density and fracture (Table 12). This success was expected since the values of the parameters used to make these two spheres were very near those of the spheres analyzed. At the same time this result demonstrates the reproducibility of the process if the parameters are controlled.

Equation 1

$$F = a_0 + a_1(HPT') + a_2(RATE')^2 + a_3(STM')(HPT') + a_4(HPP')(HPT') + a_5(STM')(RATE') + a_6(HPP')(RATE') + a_7(STM')(HPT')(RATE') + a_8(STM')(HPP')(HPT')(RATE')$$

where

F = Fracture Tendency

STM = Shard Sintering Temperature, °C STM' = STM - $\overline{STM}$

HPP = Hot Press Load, lb HPP' = HPP - $\overline{HPP}$

HPT = Hot Press Temperature, °C HPT' = HPT - $\overline{HPT}$

RATE = Load Ramp, lb/min RATE' = RATE - $\overline{RATE}$

NOTE: The last term has the greatest effect (or contribution to F).

Values of Variables		Values of Regression Coefficients	
$\overline{STM}$	= 1287°C	a_0	= 0.582
$\overline{HPP}$	= 2938 lb	a_1	= 1.587991×10^{-2}
$\overline{HPT}$	= 1559°C	a_2	= -7.055743×10^{-4}
$\overline{RATE}$	= 199.02 lb/min	a_3	= 4.097486×10^{-4}
		a_4	= -1.435635×10^{-5}
STM, HPP, HPT, RATE	= Input values for desired operating conditions	a_5	= -5.571186×10^{-4}
		a_6	= -1.108047×10^{-4}
		a_7	= 7.050789×10^{-6}
		a_8	= 4.763230×10^{-8}

Regression Equation for Calculating Fracture Tendency

Equation 2

$$D = b_o + b_1(HPP') + b_2(HPP')^2 + b_3(HPT') + b_4(HPT')^2 + b_5(RATE') + b_6(RATE')^2 + b_7(HPP')(HPT') + b_8(STM')(RATE') + b_9(HPP')(RATE') + b_{10}(STM')(HPP')(HPT') + b_{11}(STM')(HPP')(RATE') + b_{12}(STM')(HPT')(RATE') + b_{13}(HPP')(HPT')(RATE')$$

where

D = Heat Treated Density

NOTE: The cross-product terms have greater effect (or contribution to D) than the linear terms.

Values of Variables	Values of Regression Coefficients
(See Equation 1)	b_o = 0.8123 (81.23% TD)
	b_1 = 1.814357×10^{-2}
	b_2 = 3.680462×10^{-6}
	b_3 = 5.468324×10^{-2}
	b_4 = -5.963884×10^{-4}
	b_5 = 2.890933×10^{-1}
	b_6 = 5.773597×10^{-3}
	b_7 = -9.843384×10^{-5}
	b_8 = -3.187621×10^{-3}
	b_9 = 6.210994×10^{-4}
	b_{10} = -5.491211×10^{-6}
	b_{11} = 5.362572×10^{-6}
	b_{12} = -6.795091×10^{-5}
	b_{13} = -3.905227×10^{-6}

Regression Equation for Heat Treated Density

Equation 3

$$P = c_o + C_1(RATE') + C_2(STM')(HPT') + C_3(HPP')(RATE') + C_4(STM')(HPP')(HPT') + C_5(STM')(HPT')(RATE') + C_6(STM')(HPP')(HPT')(RATE')$$

where

P = As-Pressed Density

NOTE: The cross-product terms have more effect than the linear term.

Values of Variables	Values of Regression Coefficients
(See Equation 1)	C_o = 0.8224 (82.24% TD)
	C_1 = 2.572774×10^{-2}
	C_2 = -4.960912×10^{-4}
	C_3 = 9.335006×10^{-5}
	C_4 = -1.449694×10^{-6}
	C_5 = -1.812590×10^{-5}
	C_6 = -3.815194×10^{-8}

Regression Equation for As-Pressed Density

TABLE 11

Calculated Versus Observed Densities and Fracture

MHW Sphere No.	Heat-Treated Density Observed, % TD	Heat-Treated Density Calculated, % TD	As-Pressed Density Observed, % TD	As-Pressed Density Calculated, %, TD	Observed Fracture	Calculated Fracture
13	82.5	82.6	82.4	82.2	1	1.86
16	82.5	82.7	83.2	82.9	1	1.20
18	85.4	85.5	84.5	84.5	1	1.11
19	87.4	87.5	86.4	86.3	1	1.15
32	80.3	80.4	80.3	80.6	1	0.99
33	81.2	80.8	80.9	80.8	1	0.80
23	83.6	82.7	-	82.4	1	1.56
37	82.2	82.5	80.4	81.5	1	1.57
44	79.0	80.3	80.0	80.5	1	1.81
47	81.3	81.2	80.3	80.3	1	0.89
50	81.8	82.3	-	80.1	1	2.01
54	80.5	81.4	-	81.7	1	1.08
55	81.9	82.1	-	81.6	1	0.87
56	82.6	82.8	-	81.6	1	1.21
58	83.7	82.9	-	81.6	1	1.20
38	81.2	80.6	80.0	80.5	1	1.96
36	80.7	81.3	81.1	81.2	2	1.75
40	82.9	83.4	80.1	80.6	2	1.68
41	81.3	80.5	81.3	80.5	2	1.95
42	80.7	80.3	80.7	80.5	2	1.92
43	82.2	80.7	81.7	80.7	2	1.74
45	-	79.6	79.9	79.8	2	1.75
46	-	78.0	79.4	80.0	2	2.05
48	80.5	80.7	-	79.2	2	2.22
49	82.1	82.0	-	80.4	2	1.94
52	82.6	82.4	-	77.6	2	1.57
20	81.6	81.5	82.6	83.1	2	1.98
22	79.8	80.3	82.9	82.5	2	1.53
24	86.2	86.2	-	82.5	2	1.94
21	-	80.8	81.8	82.3	3	1.51
35	-	80.4	81.5	80.6	3	1.93
39	-	80.3	81.3	80.8	3	2.24
53	-	81.1	-	79.8	3	2.18
Standard error		0.83		0.63		0.61

TABLE 12

Application of Regression Equations to Post-Analysis Spheres*

MHW Sphere No.	STM, °C	HPP, lb	HPT, °C	RATE, lb/min	Calculated Density, % TD	Measured Density, % TD	Calculated Fracture	Observed Fracture
66	1315	2500	1590	241	82.67	82.4	1.26	1
67	1315	2490	1590	241	82.32	82.5	1.30	1

* See Equations 1-3.

Using Equations 1-3, contour plots have been drawn which express the variation of heat-treated density, as-pressed density, and fracture as a function of two variables with two others held constant as parameters. The plots in Figures 13 and 14 show hot press load (HPP) versus hot press temperature (HPT) with shard sintering temperature (STM) and load ramp (RATE) held constant. The load ramp was linear for the spheres described in Figure 13 and parabolic for those described in Figure 14. In both cases the slope of the ramp was calculated from a second-degree polynominal regression of the load ramp data. Only the linear term of this polynominal regression was found to correlate with sphere properties. Therefore the coefficient of this term was taken as the RATE in Equations 1-3. The values of the four variables used in both plots are typical of those for spheres made with each type of load ramp.

For each of the three sphere properties being measured (heat-treated density, as-pressed density, and fracture tendency), curves representing the maximum and minimum acceptable values for the property are drawn in Figures 13 and 14 to delineate the acceptable range. The region where these ranges converge for each property (shaded area) defines the limits for the two fabrication variables at the particular setting of the other two parameters. Spheres made within these limits should have the appropriate fracture resistance, density, and dimensions. The upper and lower limits of fracture (1 and 0, respectively) are probably conservative. The upper limit ensures no value exceeds 1.5 below which no

spheres fractured. Since values between 1 and 2 appear to be valid extrapolations, the lower limit on fracture was chosen on the assumption that the model would still be valid one unit away from 1 in either direction. Because the contours of the sphere properties are not sharply curving near the settings of the variables at which spheres were actually made, limited extrapolation to different settings of the variables is expected to give fairly good prediction of the sphere properties. The shaded areas define the maximum extrapolation.

Evaluation of Predictions of Model

Evidence that the correlations established by the statistical analysis are real and not mathematical artifacts comes from a comparison of the residual error of the model with replication error. The goodness of any statistical analysis depends on the quality of the data. In the present case, the data suffers primarily from being taken over too restricted a region and without regard to experimental design. For such data, overfitting of a model is a common problem. One usually reliable test for overfitting is to compare a measure of the residual error of the model with replicate error. In this context "residual error" refers to the difference between the predicted value and the measured value of a data point, while "replicate error" refers to the reproducibility of any data point and includes errors in parameter settings and measurements. If the model is being overfitted, then the residual error of the model will be much smaller than the replicate error. In the present analysis, for heat-treated relative density, a typical standard deviation of replicate specimens is 0.98%. By comparison, the residual error (standard error) is 0.83% indicating that overfitting is not a serious problem (R. E. Wheeler, Applied Statistics Group, Du Pont Engineering Department, private communication, May 25, 1979) and the correlations given by the model are real.

Even though the observed correlations appear to be real, the relatively high sensitivity of density and fracture to changes in key variables (as illustrated in Figure 13 by the narrow density bands and large shift of the shaded area with about 15°C change in shard sintering temperature) indicates that the production data must be accurately obtained and consistently interpreted for Equations 1-3 to be used. This is clearly shown by the hot-press-temperature measuring procedure. Accumulating vapor deposits on the view window of the optical pyrometer constantly changed the apparent temperature from one pressing to another. Tests have

shown that hot press temperature is linearly related to furnace power over the temperature range of interest (Figure 15) and the most consistent hot pressing results have been obtained by controlling to the same furnace power. Hot press temperatures used in Equations 1-3 should be obtained by converting the furnace power at temperature equilibrium using Figure 15.

In a similar way, since a 15°C change in the shard sintering temperature can make a noticeable diffrence in sphere properties, care should be taken to ensure that the sintering furnace is operating reproducibly. Data used in the present analysis was obtained from the recorder temperature with the thermocouple located at the third tray from the bottom. A 35°C correction factor was added to the indicated recorder temperature.

Explanation of Earlier High Fracture Incidence

The parametric fabrication model is useful in explaining the higher fracture incidence of Spheres 35-53, for which a parabolic load ramp was used. Figure 14 is a contour plot of hot press pressure versus hot press temperature using the same values of shard sintering temperature and load ramp as used for Spheres 41 and 42, which fractured before encapsulation. The plot shows that fracture resistances would have been better if the spheres had been pressed at lower load. This conclusion is supported by the behavior of Spheres 32 and 33, which were pressed at 3010 and 2810 lb, respectively. (The contour in Figure 14 cannot be used to support this conclusion because the ramp value was different.) Both of these spheres were rugged. Sphere 32 survived a 3 to 4-inch drop test and Sphere 33 remained unfractured through encapsulation even after storage for many months.

Further assessment of the parameters used for Spheres 35-55 indicates that the parabolic pressing ramp increases the sensitivity of sphere properties to changes in the variables over that for a linear ramp. Property control is therefore more difficult with the parabolic ramp. Greater sensitivity probably occurs because the steep slope at the end of the parabolic ramp is hard to reproduce from one run to the next. Thus, a linear ramp leads to better sphere property reproducibility and control.

As a possible other use, if the model is accurate as indicated, it can be used to back-calculate variable settings to crosscheck uncertain values to furnace calibrations.

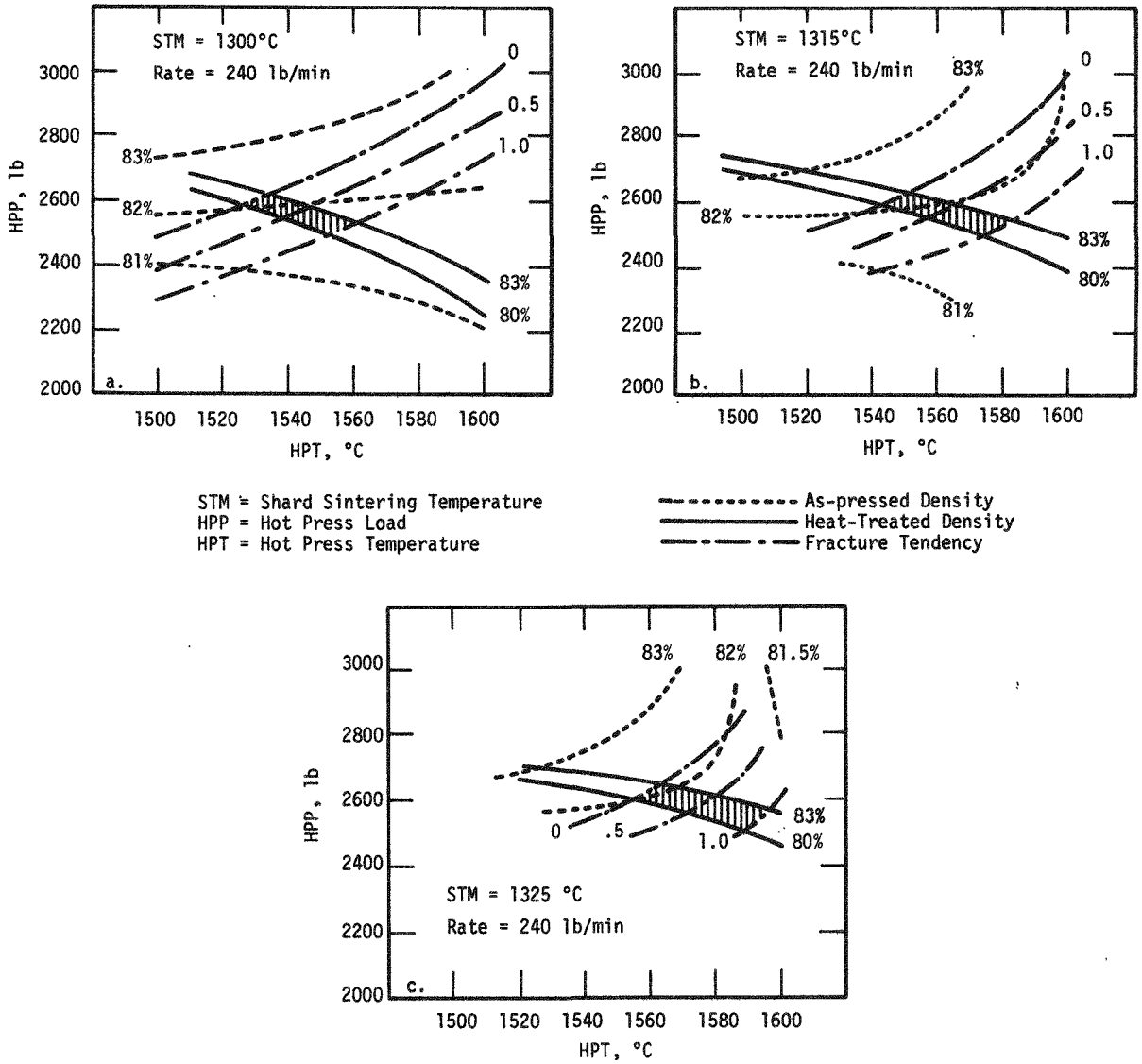

FIGURE 13. Contour Plots of Hot Press Load (HPP) versus Hot Press Temperature (HPT) for Fixed Values of Shard Sintering Temperature (STM) and Linear Load Ramp (RATE)

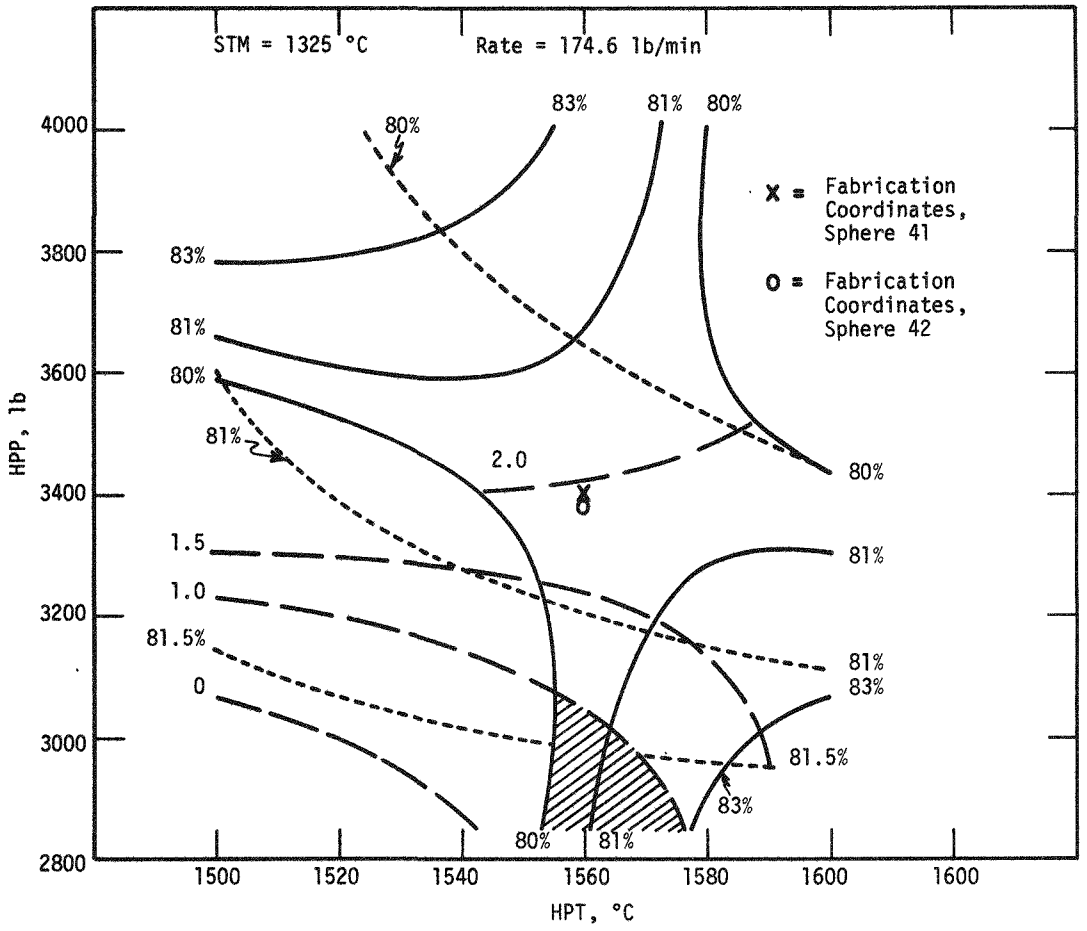

FIGURE 14. Contour Plot of Hot Press Load versus Hot Press Temperature for Fixed Values of Shard Sintering Temperature and Parabolic Load Ramp. Spheres 41 and 42.

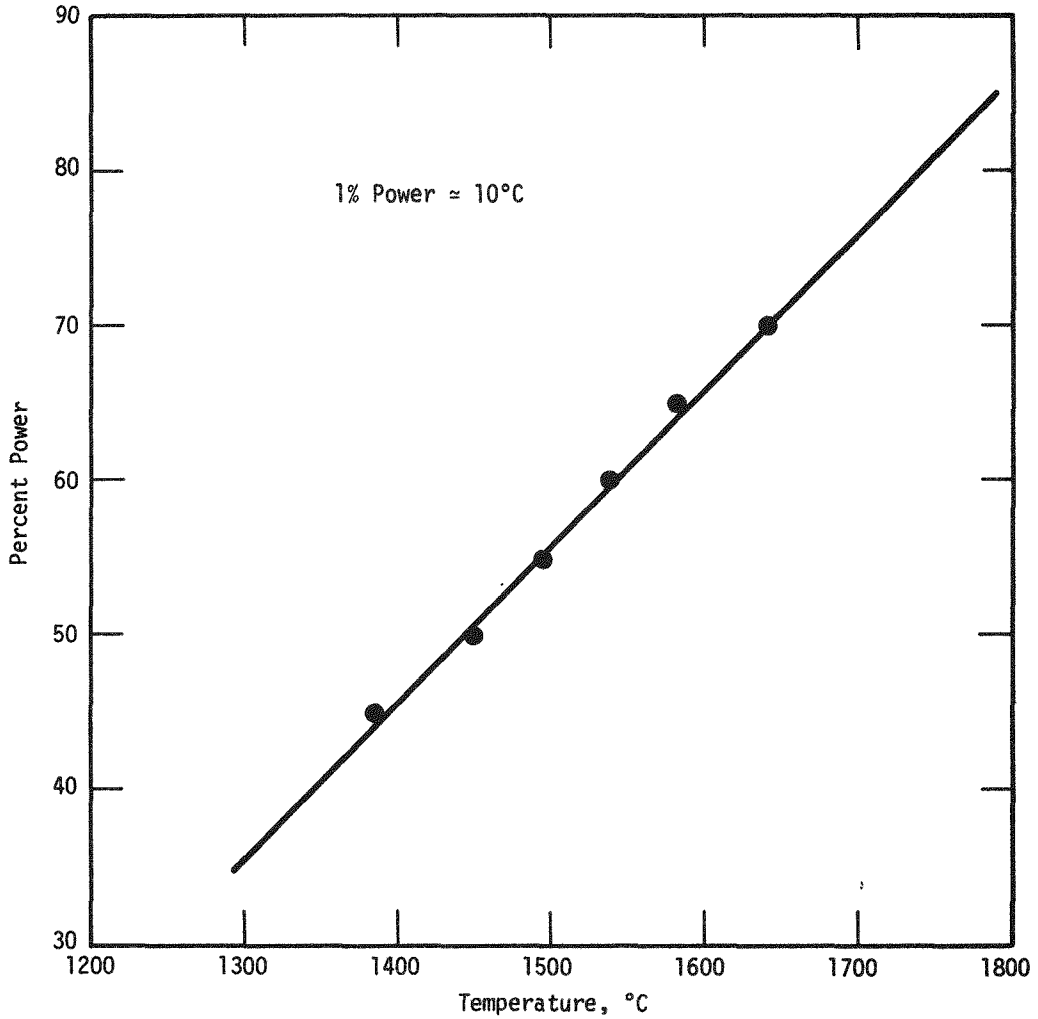

FIGURE 15. Puff Hot Press Power versus Temperature

Recommendation

On the basis of the contour plots, shown in Figures 13 and 14, we recommend that the four-key variables be run at the centerline conditions shown earlier in Table 8. If shard sintering temperature and pressure ramp are closely held to the recommended values, then the values of hot press pressure and hot press temperature place the predicted sphere properties in the middle of the acceptable range so that maximum fluctuation of hot press pressure and temperature can be tolerated and heat-treated shrinkage minimized. However, other acceptable ranges are also possible for different settings of the key variables. Consequently no one setting for the parameters can be considered exclusively optimum.

REFERENCES

1. **Savannah River Laboratory Bimonthly Report, ^{238}Pu Fuel Form Processes, March/April 1979.** USDOE Report DPST-79-128-3/4, E. I. du Pont de Nemours & Co. (Inc.), Savannah River Laboratory, Aiken, SC (1979).

2. **Savannah River Laboratory Bimonthly Report, ^{238}Pu Fuel Form Processes, January/February 1979.** USDOE Report DPST-79-138-1/2, E. I. du Pont de Nemours & Co. (Inc.), Savannah River Laboratory, Aiken, SC (1979).

3. G. L. Selman and A. A. Bourne. **Platinum Metals Review 20,** 86 (1976).